Available online at www.sciencedirect.com
SCIENCE DIRECT®
Polymer 45 (2004) 3481–3485
polymer
www.elsevier.com/locate/polymer

Creep resistant polymeric nanocomposites

Zhong Zhang*, Jing-Lei Yang, Klaus Friedrich

Institute for Composite Materials, University of Kaiserslautern, Erwin Schroedinger Str. 58,67663 Kaiserslautern, Germany

Received 23 December 2003; received in revised form 3 March 2004; accepted 4 March 2004

Abstract

In the present study, one of the unique improvements in polymer nanocomposites has been detected. Only with a very low volume fraction of inorganic nanoparticles, the creep resistance of thermoplastic could be significantly improved. 21 nm-TiO_2/PA6,6 nanocomposites were compounded using a twin-screw-extruder. The final specimens were formed using an injection-moulding machine. Static tension and tensile creep tests were carried out at room and an elevated temperature (50 °C). It was found out that the nanoparticles contributed to a remarkable reduction of the creep rate under various constant loads at both temperature levels. It is assumed that the nanoparticles restrict the slippage, reorientation and motion of polymer chains. In this way, they influence the stress transfer on a nanoscale, which finally results in these improvements.

Keywords: Polymeric nanocomposites; Creep resistance; Mechanical properties

1. Introduction

The use of thermoplastic polymers as engineering materials has become state-of-the-art. To incorporate micron-size inorganic particles into a polymer matrix is a well-known method for improving the modulus of such composites. However, a reduction in the ductility of the material may take place. Furthermore, either by diminishing the particle size or by enhancing the particle volume fraction, the flexural strength and even the tensile strength can be enhanced. On the other hand, the fracture toughness and modulus remain fairly independent of the particle size [1], even when going down to the nanoscale [2–4]. Recently, researchers demonstrated that inorganic nanoparticles could be of benefit for an increased tensile elongation [5,6]. Many researchers also reported about an increase of the glass transition temperature (T_g) of polymers by the addition of various nanoparticles, which may be due to a good bonding between the nanoparticles and the polymers, thus restricting the motion of the polymer chains [7–9]. However, the potential of property improvements of structural polymer nanocomposites is still not fully explored.

Creep is a time-dependent plastic deformation, which takes place under stresses lower than the yielding stress of materials. Recently, it was reported by Tanelke et al. [10] that nano-sized carbonitride dispersions could significantly improve the creep strength of steel at high temperatures. Relatively poor creep resistance and dimensional stability of thermoplastics are generally a deficiency, impairing the service life and safety, which is a barrier for their further expansion of application, e.g. in the automotive industry or in biomedical applications. To overcome this problem, it is shown in the present work, that even a very low volume content of 21 nm-TiO_2 particles in a polyamide 6,6 (PA6,6 or nylon6,6) matrix can remarkably improve the creep behaviour of this thermoplastic polymer under various creep loads at both room and elevated temperature. The influence of particle size and volume fraction on the property improvement was also investigated, but these results will be reported in a later paper. 1 vol.% (3.4% by weight) TiO_2/PA6,6 exhibited best performances in all the static and creep investigations, which will be concentrated in the present paper.

* Corresponding author. Tel.: +49-631-2017213; fax: +49-631-2017196.
E-mail address: zhong.zhang@ivw.uni-kl.de (Z. Zhang).

0032-3861/$ - see front matter © 2004 Elsevier Ltd. All rights reserved.
doi:10.1016/j.polymer.2004.03.004

2. Experimental

2.1. Materials

A commercial polyamide 6,6 (DuPont, Zytel 101) [11] was considered as a matrix material. TiO_2 particles (a white, dry powder of Degussa P25) were applied as fillers with a density of 4 g/cm^3 and a diameter of 21 nm. The volume content was in the range of 1% (3.4% by weight).

2.2. Extrusion

Nanocomposites were compounded using a Berstorff twin-screw-extruder (screw diameter = 25 mm, screw aspect ratio L/D = 44). Compounding was carried out at a barrel temperature of 292 °C, a screw speed of 150 rpm, and a finial extrusion rate of 9 kg/h. PA6,6 was dried in a vacuum oven at 70 °C for a minimum of 24 h before extrusion. Other processing parameters were also optimised in order to achieve a fine nanoparticle distribution in the matrix. In order to precisely control the filler content of nanoparticles, commercial K-Tron weight-controlled feeders were applied. After cooling by water bath, the extruder blanks were cut as granules with a length in a range of 3–5 mm for further injection moulding.

2.3. Injection moulding

The composites were finally manufactured using an Arburg All-rounder injection moulding machine for various specimen sharps, according to different moulds, e.g. dog-bone tensile specimens ($160 \times 10 \times 4$ mm^3, according to the German standard of DIN-ISO-527) for tensile and creep tests. The barrel temperature of the injection moulding machine was selected to be 295 °C. The injection pressure was kept constant at 500 bars, the mould temperature was fixed at 70 °C, and a constant injection speed of 80 ccm/s was applied for all specimens.

2.4. Dynamical mechanical thermo-analysis

A Gabo Eplexor® 25N Dynamical Mechanical Thermo-Analyser (DMTA) was employed to investigate the dynamic mechanical properties. Samples were cut with a length of 60 mm (40 mm in span length), a width of 10 mm and a thickness of 4 mm. Measurements were performed at tensile configuration in a sample chamber. A static pre-force of 8 N was loaded on the specimen, and an additional 10 Hz sinusoidal load with a peak value of 4 N was applied to measure the dynamic response of the specimen. The storage modulus is a function of the mean frequency (responding frequency), and the decay of amplitudes was detected as a function of time used for damping calculation. DMTA of TiO_2/PA6,6 nanocomposites were carried out in a temperature range from 110–230 °C. Liquid nitrogen was used as refrigerant for cooling the specimens down. The increase of temperature was achieved by an infrared oven in the sample chamber. Si-diodes were applied as temperature sensor.

2.5. Uniaxial tension

A Zwick universal testing machine was applied for monotonic uniaxial tensile testing. Both a 250 kN load cell and a strain gauge extensometer were equipped for measuring the tensile modulus and strength. Dog-bone tensile specimens were applied with a dimension of $160 \times 10 \times 4$ mm^3. A span length of 50 mm was considered. The crosshead speed was kept constant at 2 mm/min for room temperature and 5 mm/min for elevated temperature measurements. A temperature chamber was used for elevated temperature measurements. At least four specimens of each composition were tested, and the average values were reported.

2.6. Uniaxial tensile creep

Uniaxial tensile creep tests were preformed by a Creep Rupture Test Machine with double lever system (Coesfeld GmbH, model 2002). Ten specimens can be measured simultaneously in a testing chamber. Before testing, the desired constant load for each measurement unit was calibrated by using a force transducer. Then the samples were fixed into the clamps. For the elevated temperature measurement, the chamber was preheated to 50 °C for at least 48 h before loading was applied to the specimens in order to reach a steady temperature condition. A span length of 30 mm was marked on each specimen, and the elongation was monitored by a video camera which was equipped with a recorder and a computer image analysis system during the whole period of creep testing. The creep modulus was calculated by the ratio of the initial stress level to the measured creep stain. The measurement procedure was performed based on ASTM 2990-01 [12].

3. Results and discussions

Transmission electron microscopy (TEM) was applied to investigate the nanocomposites, and a relatively satisfactory dispersion of the nanoparticles, with a large amount of single particles, can be observed in Fig. 1. Glass transition temperatures of these materials were measured by a dynamical mechanical thermo-analysis (DMTA) approach, especially by evaluating the damping peaks. Two damping peaks at about −53 and 75 °C were observed for the neat PA6,6, which correspond to the primary- and the secondary-glass transitions, respectively. The results showed that the 21 nm-TiO_2 particles shifted both damping peaks to higher temperatures. It is a general believe that the primary-glass-transition depends on the motions of fully flexible molecular chains, and the secondary-glass-transition relies on the motions within a molecular chain. Both transitions are

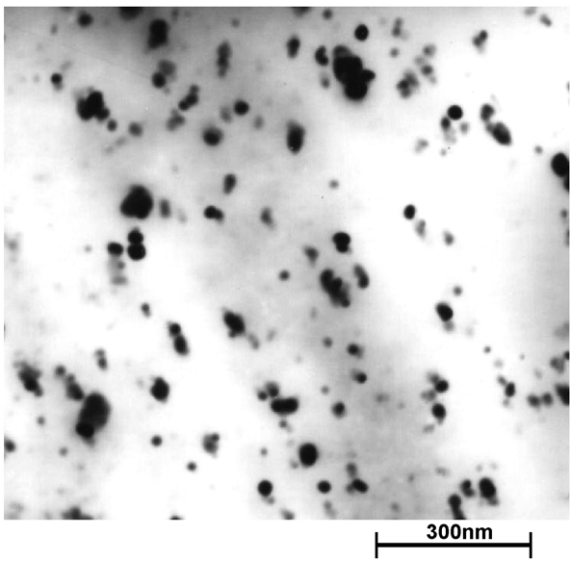

Fig. 1. Transmission electron microscopy of a 2 vol% 21 nm TiO_2/PA6,6 specimen after injection moulding.

native characteristics of polymers, which are hard to be modified by traditional reinforcing approaches. However, in the present case, the 21 nm-TiO_2 particles contributed to a more than 5-degree increase of the primary and secondary-glass transition temperatures of PA6,6, respectively.

The tensile stress versus strain curves of neat PA6,6 and 1% TiO_2/PA6,6 nanocomposite are given in Fig. 2. After a linear dependence of stress on strain at room temperature, the tensile behaviour of the neat PA6,6 was characterised by a yielding point at about 70 MPa, from where a uniform plastic deformation along the specimen length took place. Necking happened at about 23% of elongation, at which the tensile stress dropped down by about 10%, before final failure occurred at a strain of ca. 35%. No obvious necking was detected for nanocomposite. 1 vol.% of nanoparticles resulted in about the same elongation to failure, but with a slight reduction of the yielding stress and the ultimate tensile strength (UTS). Series investigations were also preformed at elevated temperatures, e.g. at 50 °C. A comparison of the tensile stress versus strain curves of the neat PA6,6 and the nanocomposite at this temperature is given additionally in Fig. 2. Both modulus and UTS were increased at elevated temperature once only 1 vol.% of nanoparticles was incorporated. On the other hand, the elongation at necking was slightly reduced.

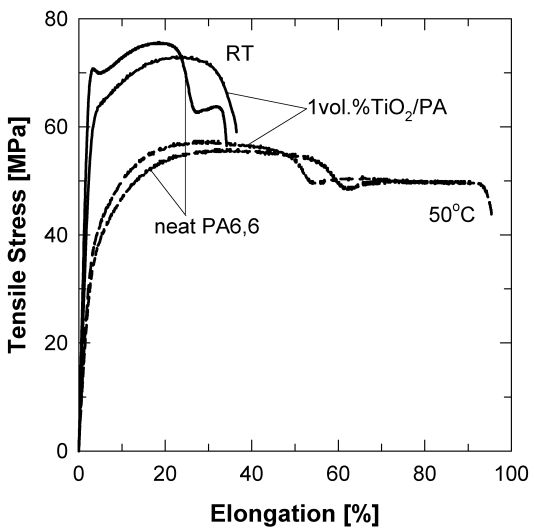

Fig. 2. Tensile stress–strain curves of neat PA6,6 and 1 vol% 21 nm TiO_2/PA6,6 composites at room temperature and 50 °C.

In addition to the static tests, creep measurements were carried out at room temperature, in which the creep stress was selected as 80% of the static UTS for each material, i.e. 60 MPa for the neat PA6,6 and 59 MPa for the nanocomposite, respectively. In general, a creep strain versus time curve can be considered as four stages (as shown in Fig. 3): (i) initial rapid elongation, (ii) primary creep, (iii) secondary creep, and (iv) tertiary creep [12]. The initial rapid elongation is due to the elastic and plastic deformation of the polymer specimen once the constant load is applied; this stage is independent of time. In the primary creep stage, the creep rate starts at a relatively high value, but decreases rapidly with time, which may due to the slippage and reorientation of polymer chains under persistent stress. After a certain period, the creep rate reaches a steady-state value in the secondary creep stage, in which normally the duration is relatively long. Finally, the material falls into the tertiary creep stage, where the creep rate increases rapidly and final creep fracture occurs.

Neat PA6,6 exhibited a relatively long creep life (more than 600 h), but at a high creep strain under this load level, as shown in Fig. 3. On the other hand, 1 vol.% 21 nm TiO_2 particles significantly reduced the creep strain of PA6,6 over all the three creep stages, although the final creep life was not very much different from that of the neat polymer under the present testing conditions. Considering the most

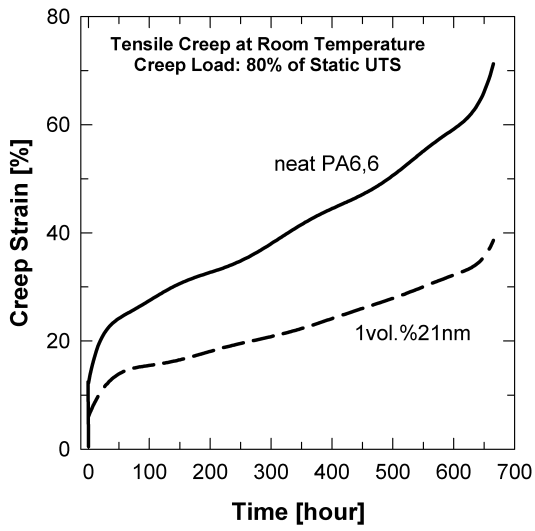

Fig. 3. Tensile creep strain vs. test duration-curves under 80% of the static UTS at room temperature. Constant creep stresses: 60 MPa for the neat PA6,6, and 59 MPa for the nanocomposite.

important creep stages separately, the nanocomposite (in spite of a slightly lower modulus and yield stress in the static tensile test) exhibited a much lower initial creep rate at the transition between the initial and the primary creep stage in comparison to the neat PA6,6. This resulted in the fact, that the creep strain boundaries for the secondary creep stage of the 1 vol%TiO_2/PA6,6 nanocomposite were at around 14 and 34%, respectively. Both were much smaller than those of the neat PA6,6, amounting to 22 and 62%, respectively. Therefore, the steady-state creep rate of the nanocomposite was about $3 \times 10^{-5}\,h^{-1}$ in the secondary stage, which was much lower than that of $6.5 \times 10^{-5}\,h^{-1}$ for the neat polymer. It is the authors' point of view that, in practice, the reduction of the creep strain is even more important for polymers than the extension of the creep life, since the former relates to the dimensional stability of the materials. The dimensional stability normally is defined as the ability of a material to maintain its size and shape under various temperatures and stresses.

The curves of creep modulus versus time in Fig. 4 release further details of the deformation process. Under 80% of the static UTS, the nanocomposite possessed a much shorter primary creep stage of only about 2 h, whereas 5–6 h were measured for the neat PA6,6. Within these time periods, a very intense modulus reduction occurred for the neat PA6,6, whereas this decrease was much smaller for the 21 nm particle filled PA6,6 system. In other words, the incorporation of smaller nanoparticles led to a much higher creep modulus in the whole range compared to neat PA6,6. This means, the load-bearing capability and the dimensional stability for the PA6,6 polymer under creep load were definitely improved by only 1 vol% TiO_2 nanoparticles.

Enhancing the creep load to 90% UTS definitely accelerated the creep process, as shown in Fig. 5. A very high initial creep rate occurred for neat the PA6,6 in the primary creep stage, which was followed by a relatively

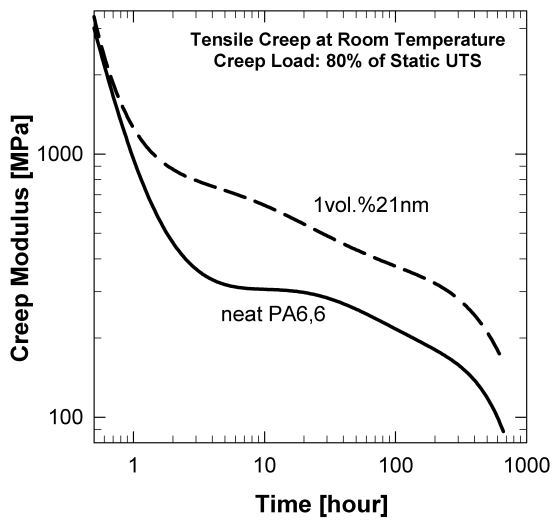

Fig. 4. Tensile creep modulus vs. test duration-curves under 80% of the static UTS at room temperature.

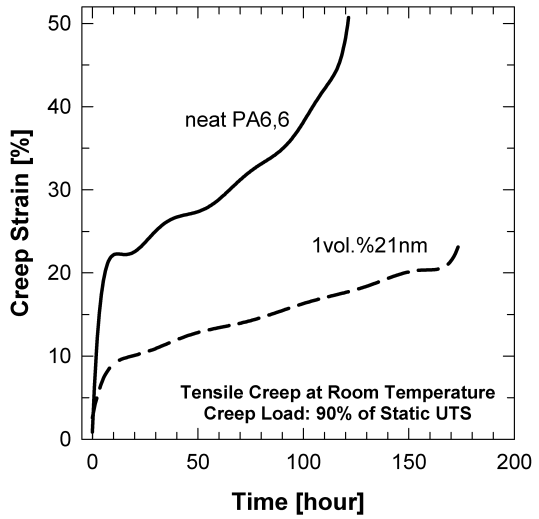

Fig. 5. Tensile creep strain vs. test duration-curves under 90% of the static UTS at room temperature. Constant creep stresses: 68 MPa for the neat PA6,6, and 66 MPa for the nanocomposite.

short secondary creep stage with a steady-state creep rate, being clearly highly than that at the lower load level. A transition to the tertiary creep stage took already place after a creep duration of 80 h only. The incorporation of nanoparticles remarkably reduced the initial creep rate in the primary creep stage. This ended up in a lower steady state creep rate within the secondary creep stage. As a result, the total creep strain was on a significantly lower level under this high creep load situation. Simultaneously, the creep life was also extended up to about 160 h. The creep modulus results confirmed this effect as well.

Creep curves of the neat PA6,6 and the nanocomposites, measured at 50 °C, are plotted in Fig. 6. The unfilled matrix was measured at two constant stresses, i.e. 50 MPa (≈90%

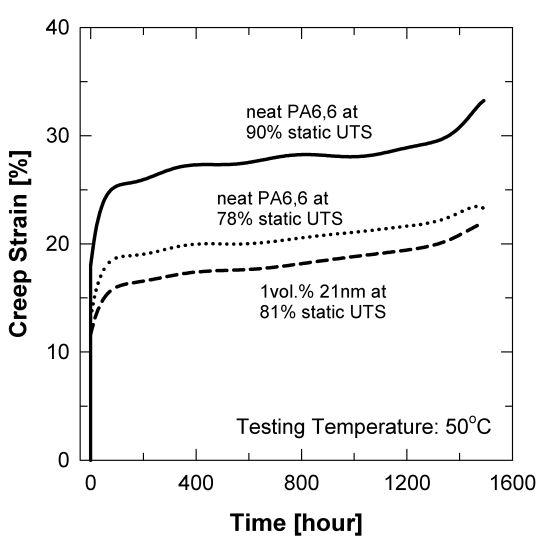

Fig. 6. Tensile creep strain vs. test duration-curves under various load levels at 50 °C. Constant creep stresses: 50 MPa (90% of UTS at 50 °C) or 43 MPa (78% of UTS at 50 °C) for neat PA6,6, and 46 MPa (81% of UTS at 50 °C) for nanocomposite.

of UTS measured at 50 °C) and 43 MPa (78% of UTS at 50 °C), respectively. The higher loading level resulted in a very high initial rapid elongation and a primary creep stage up to about 100 h. The steady-state secondary creep stage lasted more than 1200 h, thereafter, a rapid increase of the creep rate occurred in the tertiary creep stage, until the polymer fell into creep failure. A similar dependence of creep strain on time was measured for the neat polymer when loaded at 78% of UTS at 50 °C, but as expected this took place at a much lower creep strain level. The best performance was, however, found for the TiO_2/PA6,6 nanocomposite, which showed a much better creep resistance even at a high load situation, i.e. 46 MPa (81% of UTS at 50 °C). The creep modulus results confirmed again that the load-bearing capability was improved at the elevated temperature by the incorporation of nanoparticles.

4. Conclusions

In conclusion, one of the unique improvements in polymer nanocomposites has been detected. 1 vol% 21 nm-TiO_2 particles contributed to a significant improvement of the creep resistance of PA6,6 at both room and elevated temperature. The creep strain was remarkably reduced in all cases, and the creep life was extended at higher creep loading conditions (90% UTS). Nanoparticles may restrict the slippage, reorientation and motion of polymer chains. In this way, they influence the stress transfer, which finally results in these improvements. Our result should lead to improved grades of creep resistant polymer nanocomposites for engineering applications.

Acknowledgements

Z. Zhang is grateful to the Alexander von Humboldt Foundation for his Sofja Kovalevskaja Award, financed by the German Federal Ministry of Education and Research (BMBF) within the German Government's 'ZIP' program for investment in the future. The authors appreciate Prof. M.Q. Zhang, Zhongshan University of China, who kindly provided the TEM pictures. Additional thanks are due to Dr G.J. Xian and Mr H Zhang for their assistance of composite compounding.

References

[1] Moloney AC, Kausch HH, Kaiser T, Beer HR. Parameters determining the strength and toughness of particulate filled epoxide resins. J Mater Sci 1987;22:381–93.
[2] Ng CB, Schadler LS, Siegel RW. Synthesis and mechanical properties of TiO_2-epoxy nanocomposites. Nanostruct Mater 1999;12:507–10.
[3] Ng CB, Ash BJ, Schadler LS, Siegel RW. A study of the mechanical and permeability properties of nano and micron-TiO_2 filled epoxy composites. Adv Compos Lett 2001;10:101–11.
[4] Ou Y, Yang F, Yu Z. A new conception on the toughness of nylon 6/silica nanocomposite prepared via in situ polymerization. J Polym Sci, Part B-Polym Phys 1998;36:789–95.
[5] Zhang MQ, Rong MZ, Zheng YX, Zeng HM, Walter R, Friedrich K. Structure–properties relationships of irradiation grafted nano-inorganic particle filled polypropylene composites. Polymer 2001;42:167–83.
[6] Ash BJ, Rogers DF, Wiegand CJ, Schadler LS, Siegel RW, Benicewicz BC, Apple T. Mechanical properties of Al_2O_3/polymethylmethacrylate nanocomposites. Polym Compos 2002;23(6):1014–25.
[7] Becker C, Mueller P, Schmidt H. Optical and thermomechanical investigations on thermoplastic nanocomposites with surface modified silica nanoparticles. SPIE Conference on Organic–Inorganic Hybrid Materials for Photonics, vol. 3469. San Diego, California, USA: SPIE; 1998. p. 88–98.
[8] Fornes TD, Paul DR. Crystallization behavior of nylon 6 nanocomposites. Polymer 2003;44:3945–61.
[9] Sumita M, Tsukihi H, Miyasaka K, Ishikawa K. PP composites filled with ultrafine particles. J Appl Polym Sci 1984;29:1523–30.
[10] Tanelke M, Abe F, Sawada K. Creep-strengthening of steel at high temperatures using nano-sized carbonitride dispersions. Nature 2003;424:294–6.
[11] Kohan MI. Nylon Plastics Handbook. Munich: Hanser Publishers; 1995.
[12] Standard Test Methods for Tensile, Compressive, and Flexural Creep and Creep Rupture of Plastics [ASTM D2990-01] West Conshohocken, PA, ASTM International; 2001.